Tellus (1996), 48B, 487–501
Printed in UK – all rights reserved

TELLUS
ISSN 0280–6495

The earth's radiocarbon budget

A consistent model of the global carbon and radiocarbon cycles

By KEITH R. LASSEY,* *National Institute of Water and Atmospheric Research Ltd, P.O. Box 14–901, Wellington, New Zealand*, IAN G. ENTING and CATHY M. TRUDINGER, *CSIRO Division of Atmospheric Research, Private Bag 1, Mordialloc, Victoria 3195, Australia*

(Manuscript received 2 October 1995; in final form 30 June 1996)

ABSTRACT

We present the results from a global carbon-cycle model which transports 3 isotopes of carbon amongst model reservoirs. Particular emphasis is placed on the dynamics and budget of ^{14}C produced by nuclear weapons testing and augmenting natural cosmogenic production. The evolution of the "bomb ^{14}C" budget, particularly since ca. 1970, has recently been under scrutiny, and our ability to balance it been questioned. These misgivings arose from an inability to simulate simultaneously both the rising atmospheric CO_2 and the decline in its $^{14}C/^{12}C$ ratio. We use the Enting-Lassey carbon-cycle model based on a box-diffusion ocean sub-model to deduce the evolution of the budgets for both anthropogenic carbon and bomb ^{14}C, and show that these can be simultaneously reconciled with tropospheric observation. The bomb ^{14}C inventory in the model ocean is also compatible with a recent re-analysis of GEOSECS data. A key and distinctive feature of our model is the forward integration driven even-handedly by inputs of anthropogenic carbon, both from industrial sources and land use change, and bomb ^{14}C, consistently with documented emission or production patterns.

1. Introduction

Atmospheric levels of carbon dioxide (CO_2) have increased by more than 25% in 250 years due to human activities. Paramount among these activities are CO_2 releases from fossil fuel combustion and other industrial activities (Andres et al., 1996). Changes in land use have also contributed through the widespread burning of biomass and ecosystem modification. Approximately one half of the accumulated input is relocated from the atmosphere to other reservoirs, but the partitioning is uncertain. With the expectation of a continuing, if not accelerating, consumption of fossil fuels, together with forecasted climatic consequences of increasing CO_2 levels, there is a need to better understand both the cycling of CO_2 through the atmosphere and its fate. This in turn demands an understanding of the contemporary cycle of labile carbon, which would enable future trends in atmospheric CO_2 to be related to scenarios of fossil fuel consumption patterns.

Various models of the carbon cycle have been constructed to study this problem and many of these have recently been inter-compared (Enting et al., 1994; IPCC, 1995). Most such models synthesise globally aggregated information on carbon transport among key reservoirs, atmosphere, terrestrial biosphere and ocean. As a minimal requirement, such a model would adequately account for the cycling of carbon during the industrial era, ca. 1750 to present. A major obstacle to achieving this is the poor knowledge of the anthropogenic CO_2 source history, particularly the contribution from changes in land use ("deforestation").

* Corresponding author.
email k.lassey@niwa.cri.nz

There is in fact a large natural turnover of CO_2 through the atmosphere: gross fluxes of order 100 GtC/yr are exchanged with both ocean and terrestrial biosphere (1 Gt = 10^{15} g). Anthropogenic CO_2 inputs are only a few percent of these gross fluxes, and act to perturb the natural carbon cycle. Much of the information on gross carbon fluxes between major reservoirs comes from data on ^{14}C imbalance. Such imbalance is a result of human interference with the natural ^{14}C cycle which is even more substantial than with the carbon cycle itself. Prior to the industrial era the ^{14}C distribution was in near steady state, a cosmogenic production in the stratosphere balanced by radioactive decay in closely coupled reservoirs (mean life 8267 yr). Its abundance is about 1 atom per 10^{12} carbon atoms (Suess, 1955). Interference in the ^{14}C cycle takes 2 forms. Combustion of fossil fuels releases ^{14}C-free CO_2 to the atmosphere, slowly reducing by dilution the $^{14}C/^{12}C$ ratio throughout the closely coupled carbon reservoirs; this is the Suess Effect (Suess, 1955). The second and more profound interference originated from atmospheric testing of nuclear weapons which peaked in 1961–62. Intense neutron fluxes generated by the detonations transmute atmospheric ^{14}N into "bomb ^{14}C". The aggregate bomb ^{14}C production has exceeded the natural atmospheric ^{14}C inventory.

Tracking the redistribution of bomb ^{14}C has become a fruitful tool for inferring carbon-cycle dynamics, even if confounded by the ubiquitous presence of cosmogenic ^{14}C. The excess ^{14}C quickly invades the biosphere and ocean reflecting the gross (rather than net) carbon fluxes. The GEOSECS surveys of 1972–78 provide an important snapshot of oceanic bomb ^{14}C, yielding valuable information on carbon fluxes invading the oceans (Broecker et al., 1985).

In modelling the carbon cycle, all three isotopes, ^{12}C, ^{13}C, ^{14}C, can be handled as complementary tracers. This requires a knowledge of the cosmogenic production rate of ^{14}C or of its inventory in key reservoirs, and the exchange rates of ^{13}C and ^{14}C relative to ^{12}C between reservoirs — the "isotope fractionations".

There are two main limitations to employing bomb ^{14}C data to calibrate carbon-cycle models. Isotope fractionations are not always well established or depend upon environmental conditions such as temperature. But of more importance is the poor knowledge of the bomb ^{14}C budget: neither the aggregate bomb ^{14}C production nor its temporal pattern is well established. Attempts to deconvolve this budget from the tropospheric ^{14}C record raise more questions than answers (Broecker and Peng, 1994). A temporal pattern can be constructed from a history of bomb detonation yields (e.g., in Mt TNT equivalent), but with information lacking on individual detonations, independent compilations of that history rarely agree in detail. Moreover, it is also necessary to assume universal proportionality between ^{14}C production and detonation yield or similar proxy for atmospheric neutron flux.

We employ an established carbon cycle model, referred to as the Enting-Lassey (EL) model and described below, to study the perturbed carbon cycle. The perturbation is driven by constructed histories of anthropogenic inputs to the atmosphere of all three carbon isotopes. We show that the main features of observational records for carbon isotopes can be simultaneously reconciled while balancing their respective budgets, in contradistinction with some recent studies (Hesshaimer et al., 1994; Broecker and Peng, 1994). In particular we re-address issues on the bomb ^{14}C budget raised by those researchers.

2. Carbon-cycle modelling

2.1. Forward versus inverse modelling

The atmospheric CO_2 history throughout the industrial era is well established from ice core and contemporary measurement records. Because of the much poorer knowledge of the causative anthropogenic carbon inputs, the CO_2 history has commonly been specified in carbon cycle models in lieu of those inputs to drive the anthropogenic perturbation. With this "inverse modelling" approach, the history of CO_2 inputs can in principle be deconvolved from the atmospheric record. By subtracting the reconstructed history of industrial CO_2 emissions, this can yield estimates of net CO_2 inputs from the biosphere (Emanuel et al., 1984; Siegenthaler and Oeschger, 1987; Enting and Pearman, 1987; Wigley, 1993; Jain et al., 1995). Other investigators focusing on the oceanic sink of carbon have paid little or no attention to the carbon budget (Broecker et al., 1980; Siegenthaler and Joos, 1992), in some cases ignoring net exchange with the biosphere altogether

(Hesshaimer et al., 1994; Broecker and Peng, 1994).

Forward modelling, in which the causative CO_2 inputs to the atmosphere are specified and drive the anthropogenic perturbation, is less commonly applied to the industrial era. Goudriaan and Ketner (1984) performed one of the earlier comprehensive model simulations, matching the 1958–1980 atmospheric CO_2 record only approximately. Siegenthaler (1983) and Crane (1982) both prescribed an exponential approximation to the growth in industrial CO_2 emissions, ca. 1945–1980, to study net transfer to the ocean while ignoring net biospheric exchange. Craig and Holmén (1995) use forward modelling to focus on the carbon budget.

For future projections of atmospheric CO_2 levels forward modelling is driven by emission scenarios (Siegenthaler and Oeschger, 1978; Craig and Holmén, 1995; Enting et al., 1994).

Modelling the bomb ^{14}C redistribution can also be done in inverse or forward mode, analogously to and independently of CO_2. With the atmospheric record of $\Delta^{14}C$ much better established than the history of bomb ^{14}C production, almost all investigators have employed the former to drive the model's bomb ^{14}C perturbation. Of the research cited above, only Enting and Pearman (1987) and Hesshaimer et al. (1994) used the forward mode, driven by constructed histories of bomb ^{14}C production. Goudriaan and Ketner (1984) and Craig and Holmén (1995) do not address minor carbon isotopes.

To the extent that a particular empirical model incorporates a good account of carbon dynamics, inverse modelling provides useful information on the carbon and/or ^{14}C inputs. But where carbon (or ^{14}C) balance is not addressed, or where there are no independent constraints on those inferred inputs, this approach lacks the discipline that model dynamics be compatible with realistic inputs. Model simulations of gross carbon exchanges and/or of bomb ^{14}C redistribution could then be questioned.

King et al. (1992) examined the ability of several published carbon cycle models to simulate the post-1750 atmospheric CO_2 record, including projection to year 2100, when driven in forward mode by prescribed inputs. The resulting simulations exhibit wide variation and generally poor agreement with the CO_2 record, thus providing a critique of the various model structures and dynamics. Independently, Enting and Mansbridge (1987) analysed, in a model-independent manner, the relationship between ice-core CO_2 data and reconstructed anthropogenic emissions. They concluded that no linear steady-state model of oceanic CO_2 uptake could be consistent with both datasets. Enting (1992) extended this analysis to allow for CO_2 fertilisation, proposing that the anomalously high rate of CO_2 increase in the early 1800s reflected recovery from a perturbation associated with the Little Ice Age. Recent high resolution ice-core data (Etheridge et al., 1996) support this proposal. For this reason, we do not use ice-core CO_2 data from the early 19th century in our model calibration.

This paper reports, apparently for the first time, simulations in which perturbations of all three carbon isotopes are driven directly and even-handedly by constructed input histories.

2.2. *The anthropogenic inputs*

Reconstructions of anthropogenic carbon sources to the atmosphere are reported in Fig. 1. These sources drive the anthropogenic perturbation in the EL model. The industrial carbon source, devoid of ^{14}C, contains ^{13}C at levels reconstructed by Andres et al. (1996). The Houghton (1995) reconstruction of net deforestation carbon sources is published also as Table 12, Enting and Lassey (1993), and as Table A.1, Enting et al. (1994). Deforestation was evidently the larger carbon source prior to ca. 1910 (Fig. 1). Deforestation sources are the less well determined, with $\sim 30\%$ associated uncertainty.

Two independent compilations of the history of bomb detonation yields are reported in Fig. 2 as 3-monthly accumulations. Both are used in this study. That compiled by Enting (1982) to 1977, weights all surface detonations by a factor 0.5 to recognise ground absorption of half the neutron flux, while Rath (1988) compiles a full detonation history. The Enting and Rath compilations have previously been used by Enting and Pearman (1987) and by Hesshaimer et al. (1994), respectively. With each compilation is associated a best-fit 'bomb ^{14}C multiplier' (below) which scales the yield to ^{14}C production. The resulting cumulative ^{14}C production patterns differ principally up to

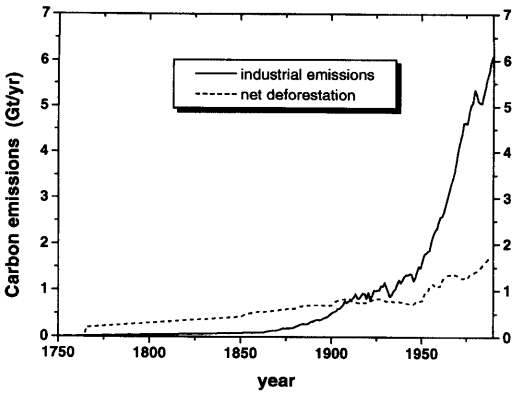

Fig. 1. The histories of anthropogenic carbon input to the troposphere, as reconstructed by Keeling (1994) and Marland et al. (1994) for industrial emissions, and by Houghton (1995) for deforestation (land use change) emissions. The industrial emissions record is extrapolated as a linear ramp from zero in 1750 to match the Keeling reconstruction commencing in 1860. The deforestation record is extrapolated as a linear ramp from 0.2 GtC in 1765 to match the Houghton reconstruction commencing in 1850, as recommended by Enting et al. (1994) in consultation with Houghton. This leaves a null deforestation record, 1750–1765.

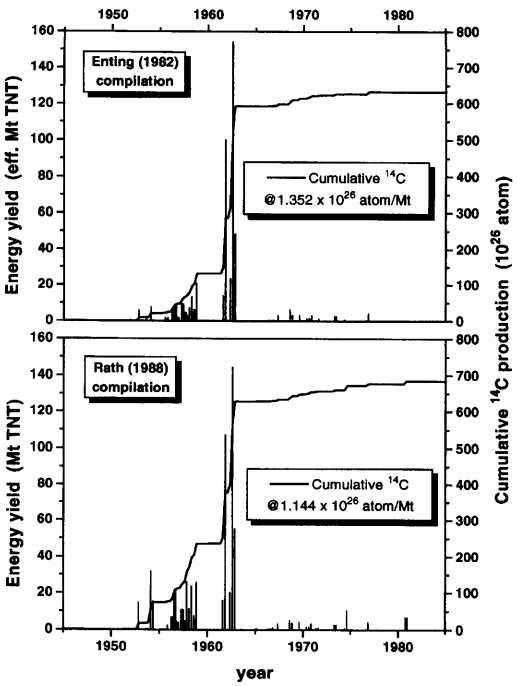

Fig. 2. The history of detonation yields from atmospheric tests of nuclear weapons, as compiled by Enting (1982) and by Rath (1988), and assembled as quarterly accumulations, are shown as bar graphs using the left-hand scale. The cumulative bomb ^{14}C production, using fitted multipliers as indicated, are shown as continuous lines using the right-hand scale. Note that the Enting compilation weights surface detonations by 0.5, and is cut off at 1977, after which Rath estimates that 6.63 Mt (TNT equivalent) were detonated.

the 1959–60 test moratorium, and in aggregate (Fig. 2).

2.3. *Bomb ^{14}C budget issues*

Two recent papers (Hesshaimer et al., 1994; Broecker and Peng, 1994) question our understanding either of the bomb ^{14}C budget, or of carbon dynamics more generally.

Using a model very similar in structure to the EL model, Hesshaimer et al. (1994), hereafter HHL, were unable to adequately simulate tropospheric $\Delta^{14}C$ during the nuclear era. In their model, the perturbation in anthropogenic carbon is driven in inverse mode by the atmospheric CO_2 record without addressing the carbon budget, while that in bomb ^{14}C is driven in forward mode by the Rath (1988) bomb detonation history with fitted multiplier. This multiplier is determined very largely by requiring the model match available stratospheric data, ca 1955–69. Atmosphere-ocean exchange is parameterised so that the model reproduces the GEOSECS bomb ^{14}C inventory of about 300 RCU* after Broecker et al. (1985). HHL found that bomb ^{14}C was transported too quickly out of the model atmosphere since 1965, and conjectured that ocean uptake of carbon might be 25% less than generally believed. While this lower uptake would appear to lend support to a smaller CO_2 exchange coefficient such as is based on the Liss-Merlivat relationship with wind speed (Etcheto and Merlivat, 1988), it would have serious repercussions for the relatively robust estimate of oceanic bomb ^{14}C at GEOSECS (Broecker et al., 1985, 1995).

* For convenience and following Lassey et al. (1990), 1 RCU (radiocarbon unit) denotes the quantity 10^{26} atoms ^{14}C; thus 1 RCU is 2.32 kg ^{14}C and 0.384 PBq of radioactivity.

Independently, Broecker and Peng (1994) assessed the year-by-year bomb ^{14}C budget by specifying the observational record in the troposphere and modelling the ^{14}C transfer to both ocean and biosphere. From the apparent ^{14}C imbalance they conjectured that unaccounted-for bomb ^{14}C must have lingered in the stratosphere until ca. 1988. However, in a more recent paper, Broecker et al. (1995) retract this proposal. They also argue that the observation-based estimate of oceanic bomb ^{14}C at GEOSECS cannot reasonably be 25% too high, and that HHL may have placed too much faith in the representativeness of pre-1965 stratospheric bomb ^{14}C measurements.

In a very recent analysis, Duffy and Caldeira (1995) suggest that a more realistic model of ocean carbon dynamics, could remedy the apparent bomb ^{14}C imbalance, as less bomb ^{14}C is transferred to their model ocean post GEOSECS than with the simple 1-dimensional ocean.

2.4. *The Enting-Lassey model*

We report simulations via forward integration using the Enting-Lassey (EL) carbon-cycle model (Enting and Lassey, 1993). This model has participated in a peer-reviewed intercomparison in support of the IPCC assessments (IPCC, 1995; Enting et al., 1994). A schematic of the EL model structure is presented as Fig. 3. The model atmosphere is represented by tropospheric and stratospheric boxes, the model biosphere by 2 boxes,

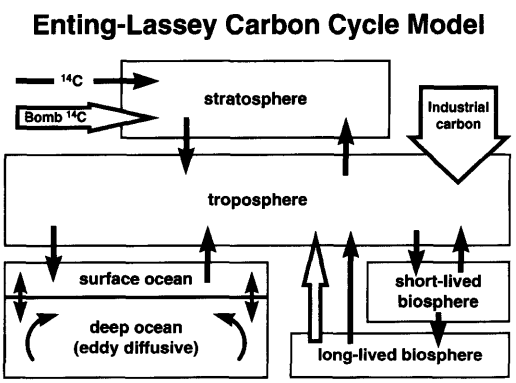

Fig. 3. The topological structure of the Enting-Lassey box-diffusion model. Solid arrows denote natural, or naturally responding, carbon flows. Hollow arrows denote anthropogenic influences: industrial carbon input, deforestation carbon transfer, and bomb ^{14}C input.

and the model ocean by an eddy-diffusive deep ocean underlying a mixed surface layer after Oeschger et al. (1975). This 1-dimensional ocean model is the basis of many studies of the carbon cycle (Siegenthaler and Oeschger, 1978; Broecker et al., 1980; Hesshaimer et al., 1994; Broecker and Peng, 1994).

The HHL model differs only in having a 3-box biosphere. There is no assurance that this greater topological complexity provides a superior simulation of carbon dynamics. Indeed, Enting (1990) has shown that the time response of the biosphere to a slug of excess ^{14}C is more influential and does not uniquely define a topological structure. Neither the HHL nor EL biospheres are founded from putative biospheric response functions.

All ^{14}C, both cosmogenic and bomb, are input to the model stratosphere which contains 15% of the atmospheric mass. The separate tropospheric and stratospheric boxes allow a delay between those inputs and their appearance in the troposphere. However, unlike HHL, we do not utilise ^{14}C measurements in the stratosphere from the early nuclear era to calibrate our model, noting that at this location and time the distribution of bomb debris would have been at its most heterogeneous.

The atmosphere-to-biosphere flux represents the net primary productivity, npp, which is viewed as a gross flux in the model. The EL model allows enhancement of npp, modelled after Allen et al. (1987) as CO_2 fertilisation. In this hyperbolic formulation, based on enhanced growth of soybeans, the npp at CO_2 concentration C is enhanced by a factor

$$G(C)=G_\infty \frac{C-C_c}{C+C_b},$$

where $G_\infty=2.40$ is the asymptotic enhancement, $C_c=80$ ppmv is the lower limit of photosynthetic activity, and C_b is set by the EL model so that $G(C_{init})=1$ with C_{init} the initial (pre-industrial) CO_2 concentration. A single free parameter specifies the extent of CO_2 fertilisation: the fraction of npp so fertilised. With a purely empirical parameterisation, CO_2 fertilisation becomes a surrogate for npp enhancement of any origin, such as anthropogenic nitrogen fertilisation. Of course, the enhanced npp is countered by enhanced decay fluxes as the biosphere strives to re-equilibrate at higher carbon content.

Ocean carbonate chemistry is characterised by a "buffer factor" which relates CO_2 partial pressure P to dissolved inorganic carbon concentration DIC. We adopt Bacastow's (1981) formulation:

$$(P-P_{ref})/P_{ref}=y\{9.36+59.56y+4558y^3\},$$

where $y=(\mathrm{DIC}-\mathrm{DIC}_{ref})/\mathrm{DIC}_{ref}$ with reference values $\mathrm{DIC}_{ref}=2.089$ mol/m^3 and $P_{ref}=290$ µatm. The buffer factor is the term in braces. Our model favours initial equilibrium of 282.9 µatm which equilibrates with 2.083 mol/m^3 through buffer factor 9.20.

With the parameter set determined — including a subset calibrated against observational data (Subsection 3.2) — the model is integrated through time from an initial pre-computed steady state in 1750. This initial state is characterised by a CO_2 mixing ratio and its ^{13}C content, and by the cosmogenic ^{14}C production rate. The values for initial CO_2 and for cosmogenic ^{14}C production are determined as part of the calibration process. At each time step, industrial carbon is injected into the model troposphere and deforestation carbon relocated there from the long-lived biosphere, according to the inputs of section 2.2. Both cosmogenic and bomb ^{14}C are injected into the model stratosphere. Each of the three isotopes, ^{12}C, ^{13}C and ^{14}C, is redistributed among the reservoirs, and a fraction of the ^{14}C removed as radioactive decay.

Houghton's (1995) constructed deforestation fluxes account not only for destruction of standing biomass and its transfer (over various time scales) as CO_2 to the atmosphere but also for reverse forest recovery processes such as regrowth (Appendix A.6, Enting et al., 1994). The EL model requires a gross carbon transfer (Fig. 3), generating its own return fluxes as a natural return toward carbon equilibrium. We therefore first construct a model-dependent gross flux, $D(t)$, from Houghton's record of net flux, $B(t)$:

$$D(t)=B(t)+\lambda_L\int_{1750}^{t}B(t')\mathrm{d}t',$$

where λ_L is the inverse turnover time of the long-lived biosphere. The net effect of this constructed gross flux is to change the carbon content of the long-lived biosphere at the rate $B(t)$: see Enting and Lassey (1993) for more detail.

3. Numerical experiments

3.1. Numerical strategy

We present two formulations of the EL model, referred to as experiments $F+D$ and F, each with 2 variants, E and R, corresponding to the bomb ^{14}C record of Enting (1982) and of Rath (1988); we denote the variants as $F+D/R$, etc. Experiment F drives the carbon cycle with the industrial emissions history of Fig. 1, maintaining null net exchange of carbon with the biosphere (but not of carbon isotopes separately). Experiment $F+D$ additionally admits deforestation and fertilisation fluxes, the former from Fig. 1, the latter parameterised after Allen et al. (1987). All experiments are forward integrated from a 1750 steady state to 1990.

Experiment F/R can be compared directly with HHL who, like many others (Crane, 1982; Siegenthaler, 1983; Broecker and Peng, 1994), neglect biospheric destructive and fertilised fluxes. The biosphere is then a spectator in net carbon dynamics, but not in net ^{13}C or ^{14}C dynamics. With a spectator biosphere throughout the entire industrial era, we find that Experiment F needs an artificially elevated initial CO_2 to compensate for the lack of deforestation sources.

Table 1 and Fig. 4 present the parameter set

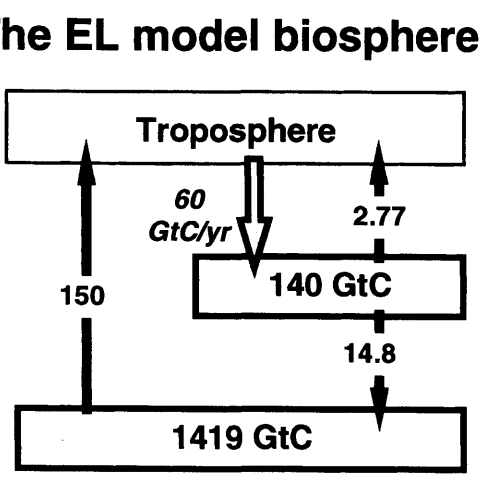

Fig. 4. The biospheric component of the Enting-Lassey model at pre-industrial equilibrium. The numbers overlaying the arrows denote the e-folding times in years corresponding to those fluxes. The hollow arrow represents the flux of npp.

Table 1. *Fixed parameters used in the EL model*

ocean depth (surface layer) (m)	75*
ocean depth (total) (m)	3800*
ocean surface area (10^{12} m^2)	361.2
deep ocean diffusivity (m^2 yr^{-1})	7685*
tropospheric C turnover w.r.t. ocean (yr)	7.80*†
net primary productivity (GtC/yr)	60*
atmospheric CO_2 burden (GtC/ppmv)	2.1276
troposphere : stratosphere mass ratio	85 : 15*
stratospheric C turnover time (yr)	2.50*
cosmogenic ^{14}C production (RCU/yr)	2.45
bomb ^{14}C production (E) (RCU/eff. Mt TNT)	1.352
bomb ^{14}C production (R) (RCU/Mt TNT)	1.144
isotope fractionation factors (^{13}C/^{12}C)‡:	
atmosphere – ocean	0.99795
ocean – atmosphere	0.99005
atmosphere – biosphere	0.98200
biosphere – atmosphere	1.00000

* Parameter value matches that adopted by HHL.
† Equivalent to a CO_2 invasion rate of 0.0629 mol/m^2-yr-μatm.
‡ ^{14}C/^{12}C fractionation factors are the square of those for ^{13}C/^{12}C.

common to experiments *F*, *F* + *D*. Where possible and appropriate, values are specified to match those of HHL, others are calibrated by Bayesian techniques, and the remainder are computed to assure initial equilibrium. Of the biospheric parameters, we specify the size of the short-lived biota, calibrate the size and turnover of the long-lived biota, and compute the remainder to equilibrate with the prescribed npp.

3.2. *Model calibration*

The values of selected model parameters are prescribed by calibrating against observation using the Bayesian technique. This technique is fully described by Enting and Pearman (1987) and by Enting and Lassey (1993). Calibration merely fine tunes parameter values that would otherwise be judgementally selected as "reasonable", by optimising the model's simulation of a carbon-cycle "observation set" (such as CO_2 mixing ratio, Δ^{14}C value, at specified times) while constraining the excursions of parameter values from "prior estimates". This involves iteratively running a full simulation within an optimisation scheme which minimises a sum of squares of weighted differences, both between each observational datum and its simulation, and between each tuneable parameter and its prior estimate. With each datum in the observation set and each tuneable parameter is associated an adjudged uncertainty whose inverse square is used as a weight in the optimisation scheme.

It should be emphasised that calibration is an off-line parameter specification process which cannot assure the model's exemplary simulation of the observation set deployed. Rather, it should be thought of as minimising their mismatch.

The observation set that we adopt comprises the following: 21 tropospheric CO_2 data throughout 1887.5–1986.5, with greater weight on the post-1958 Mauna Loa record; 4 Δ^{14}C data for the short-lived biosphere, 1805–1950; 2 ocean-surface Δ^{14}C values, 1955 and at GEOSECS; 1 abyssal ocean value for Δ^{14}C at GEOSECS; 3 tropospheric Δ^{14}C values, 1967.5–1974.5. The tropospheric CO_2 dataset, taken from the sources of Fig. 5, deliberately excludes ice-core data before 1887. This is both because of the uncertainty in emissions reconstructed for this era (deforestation sources are dominant, and are extrapolated back from 1850 without corroborative data: see Fig. 1), and because pre-industrial carbon distribution may not have been equilibrated as noted in Subsection 2.1. The biospheric Δ^{14}C represents carbon photosynthesised at those times and subsequently assimilated into tree rings, and is taken from the tree ring analyses of Lerman et al. (1970). These values enable the model cosmogenic ^{14}C strength to be fine-tuned by the Suess Effect. The

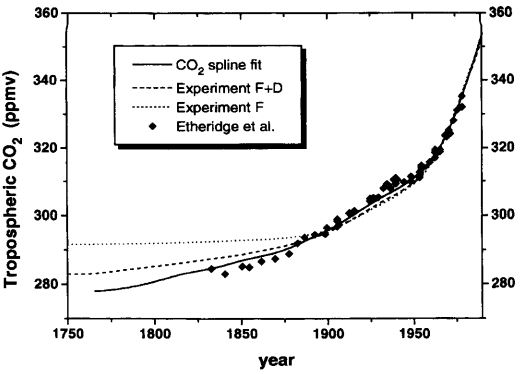

Fig. 5. The CO_2 record as simulated by experiments $F+D$ and F, compared with the observational record. The solid line denotes a spline fit to the combined Mauna Loa and ice-core records as used to support the IPCC inter-comparison (Enting et al., 1994) with data sourced from Keeling et al. (1989), Neftel et al. (1985), Friedli et al. (1986). Post-1887 data from this record are used to calibrate model parameters. The recent data of Etheridge et al. (1996) combined from 3 Antarctic ice-cores is also shown.

oceanic $\Delta^{14}C$ data, taken from Broecker et al. (1960, 1985), tune the ocean response to the nuclear signal. Finally, the tropospheric $\Delta^{14}C$ data average northern and southern hemisphere time series (Levin et al., 1985; Manning et al., 1990) up to GEOSECS time only, and primarily tune the bomb ^{14}C multiplier. The reason for this cut-off is to establish whether, unlike HHL, our model can simulate the post-1975 $\Delta^{14}C$ record unconstrained by any post-1975 data other than CO_2.

The above observation set, which has much in common with that used by Enting and Pearman (1987), reflects our judgement of the best-determined carbon cycle observations which a model as simple as EL can be expected to simulate. We tune values of only those parameters for which the HHL values either are inapplicable (biospheric parameters, initial CO_2) or prove inappropriate (^{14}C source strengths).

We adopt the following strategy for Bayesian calibration of our numerical experiments.

(1) Tune 6 model parameters to optimise expt $F+D/R$ against the observation set. The 6 are: initial atmospheric CO_2; cosmogenic ^{14}C production rate; CO_2 fertilisation extent; size and turnover time of the long-lived biosphere; bomb ^{14}C multiplier (R compilation).

(2) Tune the bomb ^{14}C multipier for $F+D/E$ by substituting the E bomb ^{14}C compilation for the R compilation, leaving all other parameters unchanged.

(3) For expt F/R, retune only the initial CO_2 while ignoring deforestation and fertilisation fluxes, and retaining all other parameter values of step 1. Further recalibration provides little further improvement. For expt F/E the bomb ^{14}C multiplier of step 2 is substituted without further calibration.

The optimised initial atmospheric CO_2 is 282.9 ppmv for expt $F+D$, and 291.7 ppmv for expt F. The former value is near the 279 ± 3 ppmv suggested by ice-core data (Neftel et al., 1985). The more elevated latter value compensates for the absence of deforestation carbon, and is close to values adopted in other investigations which ignore deforestation fluxes (e.g., 290 ppmv by Crane (1982); 292 ppmv by Broecker and Peng (1994)). Without this compensation, expt F cannot adequately simulate the contemporary CO_2 record, as noted also by King et al. (1992). Nevertheless, HHL use that CO_2 record to drive the industrial-only anthropogenic perturbation from an initial 280 ppmv.

For expt $F+D$ npp is enhanced quite significantly from the initial 60 GtC/yr to 72.4 in 1990. Return fluxes are correspondingly elevated with the result that the net model-driven storage is 1.95 GtC/yr in 1990 (countered by Houghton's 1.71 GtC/yr deforestation net of regrowth). This compares favourably with estimates of net storage for the 1980s attributed to CO_2 fertilisation by Schimel (1995) at around 1 GtC/yr and by IPCC (1995) at 0.5 to 2.0 GtC/yr. That such a large enhancement in npp is needed to generate a modest net storage may in part be an artefact of the simple model biosphere which lacks a long-term sequestration compartment such as soil carbon.

The optimised cosmogenic ^{14}C production rate of 2.45 RCU/yr (or 1.52 atom/cm^2/s) is at the low end of independent estimates of this parameter, but still exceeds the 2.3 RCU/yr adopted without comment by HHL. O'Brien (1979) estimates that the contemporary inventory could be sustained by a production rate of 1.75 atom/cm^2/s, while Stuiver and Quay (1980) assess that between 1.6 and 1.9 atom/cm^2/s would be required. That the model-preferred cosmogenic production rate

Table 2. *Pre-industrial equilibrium of carbon isotopes calculated by EL model, experiment* F+D

	Total C (Gt C)	$\delta^{13}C$ (‰)	^{14}C (RCU)	$\Delta^{14}C$ (‰)
troposphere	512*	−6.40*	314	0.65
stratosphere	90*	−6.40*	62	110.94
ocean surface	677†	1.53	402	−48.13
ocean, deep	33635†	1.53	18571	−145.14‡
biosphere, short	140*	−24.28	83	0.56
biosphere, long	1419*	−24.28	824	−17.28
total	36473		20255	

* Prescribed input to the model.
† Equivalent to concentration of 2.083 mol m^{-3}.
‡ In abyssal ocean.

might be low suggests that the model's carbon reservoirs that are coupled to the atmosphere with exchange times up to ~10,000 years may be too small. A major culprit may well be the simple eddy-diffusive model ocean which cannot support a near-constant ^{14}C concentration, $\sim 1.4 \times 10^{12}$ atom/m^3, observed at depth (Fairhall and Young, 1985). The global ^{14}C inventory consistent with a production of 2.45 RCU/yr is about 20,300 RCU, apportioned according to Table 2. An independent compilation of the oceanic inventory of cosmogenic ^{14}C is 19,700 RCU, excluding the marine biosphere (Lassey et al., 1990).

The optimised bomb ^{14}C multipliers are 1.352 RCU per effective Mt TNT for the Enting compilation, and 1.144 RCU per Mt TNT for the Rath compilation. For these 'E' and 'R' bomb ^{14}C records, respective aggregate ^{14}C productions are 632 and 684 RCU, the former only to 1977 (after which about 9 RCU would have been generated from 6.6 Mt detonations). Significantly, with the R record 236 RCU is produced prior to the 1959–1960 moratorium, compared to only 104 RCU with the E record. Actual total production can be estimated independently by aggregating separately-assessed inventories in major reservoirs, each having its attendant uncertainty. The most recent such estimate is 670 RCU (Broecker et al., 1995). Note that HHL adopt a multiplier 1.00 RCU/Mt with the Rath compilation (V. Hesshaimer, personal communication, 1995) based largely on matching the sparse stratospheric record during ca. 1955–1969; this implies aggregate production of 598 RCU.

It is clear that HHL cycle significantly less ^{14}C, both cosmogenic and bomb, through their model reservoirs than we do. This is a key distinction between the parameterisations.

4. Results

Model simulations are summarised in Figs. 5–9 and Tables 2–4. It is immediately clear that, unlike HHL, we are able to simultaneously match both the rise in atmospheric CO_2 and the main features of its $^{14}C/^{12}C$ ratio throughout at least the 20th century.

While the simulated record of tropospheric CO_2 is quite good for the 20th century, especially

Table 3. *Model carbon fluxes (GtC/yr) in 1990, experiment* F+D

gross: atmosphere – ocean	96.06
gross: ocean – atmosphere	93.60
gross: atmosphere – biosphere	72.38
gross: biosphere – atmosphere	72.14
net: atmosphere – ocean	2.46
net: atmosphere – biosphere	0.24
deforestation – atmosphere	1.71
industrial emissions	6.08
net atmospheric accumulation	3.38

Table 4. *Ocean ^{14}C inventory changes (RCU) as at 1 January*

Experiment	1750–1975	1950–1975	1750–1990
F+D/E	338	329	445
F/E	324	332	432
F+D/R	368	359	482
F/R	354	362	469

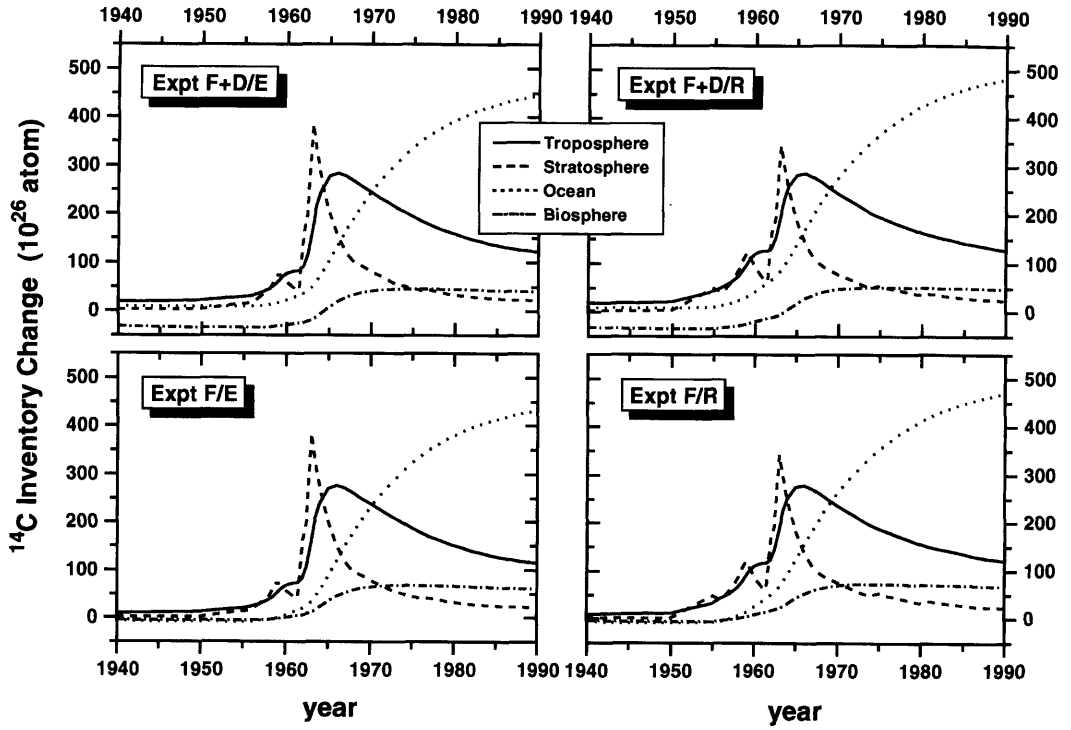

Fig. 6. The changes in reservoir ^{14}C inventories since 1750, as simulated by experiments $F+D$ and F, each with the E and R bomb ^{14}C records.

post-1950 (Fig. 5), systematic departures are evident at earlier times, particularly for expt F. For expt $F+D$ the departure may be a result of an over-simplified model biosphere, errant deforestaton releases (the Houghton construction has $\sim$30% uncertainty post-1850, and lacks firm data to support pre-1850 extrapolation), and/or a Little Ice Age recovery as noted in Subsection 2.1 and by Enting (1992).

Table 3 reports the carbon flux imbalance in 1990 for expt $F+D$, showing an atmospheric accumulation rate of 3.38 GtC/yr, or CO_2 growth of 1.59 ppmv/yr. It is noteworthy that the model biosphere is almost in transient equilibrium with the atmosphere since the 1960s as the enhanced npp assists recovery from cumulative deforestation losses (see also Fig. 8), vindicating the oft-assumed "spectator biosphere" during the nuclear era. The ocean is then the dominant carbon sink (2.46 GtC/yr). With no climate feedbacks the EL model can simulate only general trends and cannot mimic the strong interannual variations observed in the carbon cycle since the 1980s (Francey et al., 1995; Keeling et al., 1995). But if the real terrestrial biosphere of recent decades is, on average, also close to equilibrium, then relatively small year-by-year changes in npp of order 1 GtC/yr will equate directly to changes in net biospheric sink (because biospheric return fluxes could not instantly respond). Npp changes of such magnitude can then profoundly influence the relative and combined roles of biosphere and ocean as net carbon sinks.

The simulated change in oceanic ^{14}C inventory, 1950–1975, can be compared with independent estimates of bomb ^{14}C at GEOSECS: Tables 4, 5. While the former appear somewhat larger, some elaboration of both tabulations is required. Firstly, for a common bomb detonation record (Rath, 1988), expt F/R cycles 14% more bomb ^{14}C than HHL's model, and this in turn results in a 14% greater invasion of bomb ^{14}C to the ocean (since both models are characterised by the same invasion rates). As a result, our oceanic inventory at

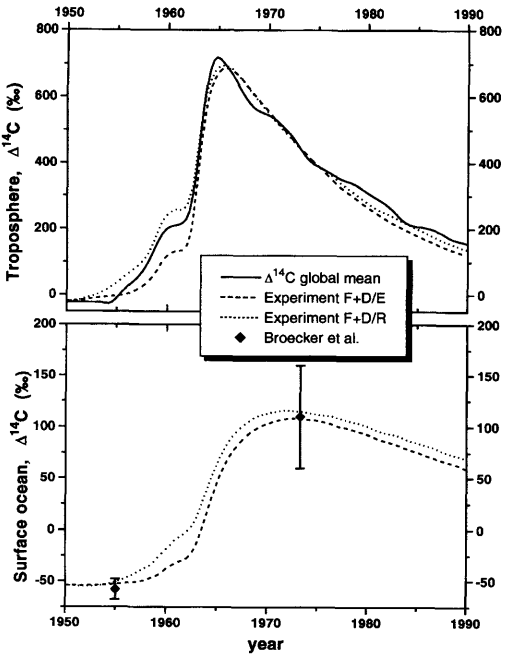

Fig. 7. Simulated $\Delta^{14}C$, 1950–1990, in the troposphere (upper panel) and surface ocean (lower panel) for experiment $F+D$ with both E and R bomb records. The corresponding simulations for experiment F are indistinguishable. The upper panel also includes the globally-averaged observational record, as supplied by M. Heimann in support of the IPCC inter-comparison (Enting et al., 1994), with main sources Levin et al. (1985), Manning et al. (1990) for the two hemispheres. Data from this record, 1967–1975, are used to calibrate model parameters. The lower panel includes two observational data, a pre-GEOSECS Atlantic average (Broecker et al., 1960), and a composite value based on the GEOSECS programme (Broecker et al., 1985).

Table 5. *Independent ocean ^{14}C inventory estimates (RCU) at Geosecs*

Broecker et al. (1980)	314
Broecker et al. (1985)	289
Lassey et al. (1990)	303
Broecker et al. (1995)	305

GEOSECS exceeds by ~14% the 300 RCU to which HHL's model is constrained (1 January 1974). Thus the inventory changes in Table 4 result directly from our decision to retain HHL's ocean parameterisation rather than to fit the 1974 bomb ^{14}C inventory as per HHL. Secondly, meas-

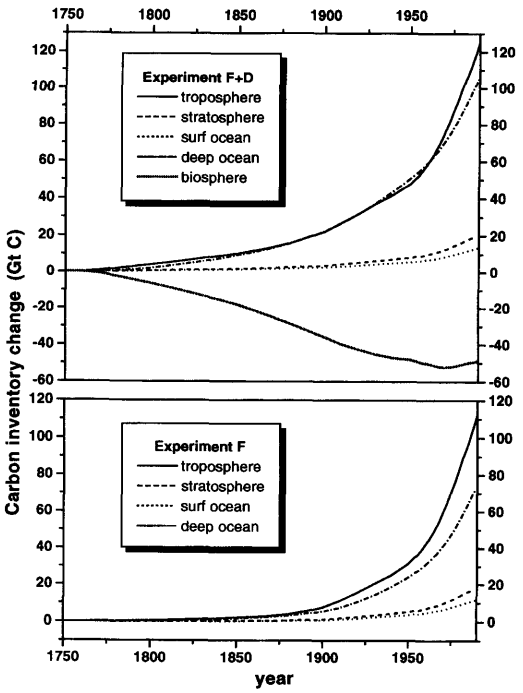

Fig. 8. The changes in reservoir carbon inventories since 1750, as simulated by experiments $F+D$ and F. Both panels have the same scales.

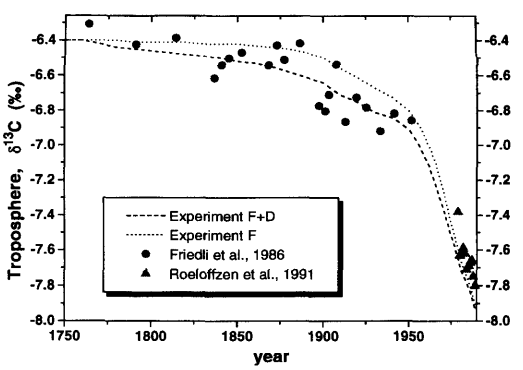

Fig. 9. The tropospheric $\delta^{13}C$ trend as simulated by experiments $F+D$ and F, commencing at a prescribed −6.4‰ in 1750. The ice core determinations from Antarctica of Friedli et al. (1986) are shown, together with contemporary measurements from Mauna Loa by Roeloffzen et al. (1991).

urement-based estimates are complicated by the protraction of the GEOSECS surveys over about 6 years, 1972–8, during a time of rapidly changing bomb ^{14}C distribution. Those of Table 5 adjust for that protraction. Broecker et al. (1980) identify their estimated 314 ± 35 RCU with year 1973. The date associated with the more comprehensive inventory of 289 RCU (Broecker et al., 1985) is unclear — probably 1972–3 of the Atlantic survey. The estimate of 303 RCU by Lassey et al. (1990) merely corrects the latter $\Delta^{14}C$-based estimate for one correctly based on $\delta^{14}C$. In the most recent estimate of 305 RCU for 1975.0, Broecker et al. (1995) correct a "bulk" estimate of 331 RCU by 8% for the effect of regions where shallow water limits bomb ^{14}C penetration. Since both the EL and HHL ocean sub-models have uniform ocean depth exceeding that of bomb ^{14}C penetration, it might be reasonable to expect such models to overestimate the delivery of bomb ^{14}C to the ocean. Thus the 1950–75 inventory of Table 4, especially the E variants, may well be appropriate for the model.

The evolutions of the bomb ^{14}C inventories are qualitatively similar for the four simulations (Fig. 6). The R bomb ^{14}C record has relatively more pre-1961 production, and this is reflected in the simulated stratospheric and tropospheric inventories. Much of the greater ^{14}C production associated with the R record is transferred to the model ocean by ca. 1961 to result in a GEOSECS-era ocean inventory systematically higher than with the E record and therefore further from independent estimates (Table 5).

The main features of the tropospheric $\Delta^{14}C$ record are well simulated throughout the nuclear era (Fig. 7). That this simulation for 1965–1975 is slightly superior than for 1975–1990 reflects a calibration procedure which leaves the latter period unconstrained. A smaller post-1975 transfer to the ocean which Duffy and Caldeira (1995) suggest would accompany a more realistic model ocean would improve the tropospheric fit.

The observational record reported in Fig. 7 is the mean of only two available, one for each hemisphere. It is fortunate that both these records start as early as 1955, pre-dating the main bomb ^{14}C production. The largest discrepancies between experiments $F+D/E$ and $F+D/R$ are in the 1955–61 period when the observational record quite neatly bisects them. While this could suggest that the actual bomb ^{14}C productions lie between the constructed E and R records, it should be recognised that spatial distributions of ^{14}C would have been at their most heterogeneous during the time of rapid ^{14}C growth, and also that some of the bomb ^{14}C may have been deposited directly in the troposphere.

Fig. 8 provides the counterpart of Fig. 6 for total carbon. A particular feature is the recovery from decline of the simulated biospheric reservoir in expt $F+D$ commencing ca. 1970, as noted above. While expt $F+D$ exhibits a greater accumulation of anthropogenic carbon in both atmosphere and deep ocean than expt F, this is an artefact of the latter's artificially elevated initial CO_2 which results in a proportionately lower CO_2 increase, 1750–1990.

Fig. 9 shows the simulated decline in $\delta^{13}C$ of tropospheric CO_2 from a prescribed initial $-6.4‰$, and its concordance with observation. Including deforestation fluxes would appear to assist this concordance. This provides some confidence that isotope signals are propogated through the model more or less correctly, noting that we calibrate no model parameters affecting ^{13}C transport independently of ^{12}C transport.

5. Discussion and summary

5.1. Comparison of experiment F/R with HHL

The key distinctions between the HHL and our model strategies are 3-fold.

Firstly, driving both carbon and ^{14}C perturbations even-handedly from prescribed atmospheric inputs assures a formulation of carbon isotope dynamics that is internally consistent with realistic budgets. HHL adopt the more widely-used approach of prescribing the history of atmospheric CO_2 in lieu of that of industrial carbon emissions, and complement this with a prescribed history of ^{14}C inputs. With a formulated carbon exchange between atmosphere and ocean, and null exchange between atmosphere and biosphere, there is no assurance that the history of atmospheric inputs required to close the carbon budget is realistic.

Secondly, whereas HHL's selection of "bomb ^{14}C multiplier" hinges pivotally on stratospheric ^{14}C data from 1955–1966, we disregard these data in favour of a mainly tropospheric ^{14}C dataset to

1975, resulting in a multiplier larger by 14% and proportionately greater bomb ^{14}C production. Both Lassey et al. (1990) and Broecker et al. (1995) have noted the likely heterogeneity of stratospheric ^{14}C concentrations during a measurement period characterised by major detonations.

Finally, our model formulation requires significantly greater generation of both cosmogenic and bomb ^{14}C (by 6% and 14%) than HHL adopt, with both being closer to independent estimates. The greater bomb ^{14}C production is accompanied by its proportionately greater oceanic invasion up to GEOSECS time (when cumulative bomb ^{14}C evasion remains minor). Had HHL cycled more bomb ^{14}C and still required a match to the GEOSECS ocean ($\sim$300 RCU in 1974), bomb ^{14}C would have persisted longer in the atmosphere, at the expense of lower uptake of industrial carbon by the ocean.

A useful comparison can be made between the bomb ^{14}C budget for expt *F/R* and 114% of that budget for HHL's model (denoted 1.14*HHL). Of the common 1990 inventory of 684 RCU, F/R and 1.14*HHL apportion it as 131+479+74 and 72+476+136, respectively, for atmosphere+ocean+biosphere. (We are identifying the reservoir inventory of bomb ^{14}C with the ^{14}C inventory in 1990 less that in 1950). It is clear that the bomb ^{14}C "missing" from the 1.14*HHL atmosphere is to be found in the biosphere. Both models have identical formulations of biospheric as well as of oceanic uptake, so it is the return fluxes from the biosphere that must account for the above difference. We thus revisit the respective biospheric response functions: a comparison of these reveal a faster turnover for F/R, so that the dominant bomb ^{14}C "pulse" of ca. 1962 returns more quickly to the atmosphere. Indeed, after 28 years (viz, 1962–1990) only 12% of an idealised pulse would still reside in the *F/R* biosphere compared to 20% for HHL, which is approximately the ratio noted above for bomb ^{14}C residing in the F/R and 1.14*HHL biospheres.

While there are no objective criteria at present to favour one biospheric representation over the other, we note that the formulation of the EL biosphere has been tuned to exogenous information, whereas the HHL biosphere is apparently uncalibrated.

5.2. Conclusions

Contrary to recent findings by HHL and by Broecker and Peng (1994), the global budgets of anthropogenic carbon and of bomb ^{14}C are compatible with each other and with simple models of the carbon cycle, provided the model formulation recognises that CO_2 sources to the atmosphere be compatible with carbon dynamics and a balanced carbon budget.

By driving perturbations in both total carbon and ^{14}C with prescribed histories of atmospheric input, all three isotopes can be cycled with even handed dynamics. This enables all three isotope budgets to be automatically in balance with realistic inputs.

We propose that the HHL model cycles insufficient cosmogenic and bomb ^{14}C. This suggests that their global inventory of labile carbon accompanying the cosmogenic ^{14}C may also be too low. Furthermore, the HHL biosphere may be ill-tuned, resulting in insufficiently fast carbon turnover.

With bomb ^{14}C production history poorly determined, we have deployed two independent compilations, each with a multiplier scaled to fit selected data. These suggest surprisingly different accumulations of bomb ^{14}C. In particular, the Rath (1988) compilation favours much greater ^{14}C production prior to the 1960 test moratorium leading to 8% more production overall. Fig. 7 suggests that reality may lie between these two compilations, while the modelled oceanic ^{14}C during GEOSECS favours Enting's (1982) compilation.

6. Acknowledgements

We are grateful for useful discussions and data exchanges between KRL and Dr Vago Hesshaimer, enabling a careful comparison of the HHL and EL models. Dr T-H Peng (NOAA/AOML, Miami) provided some clarification of his work with Dr Broecker. We also thank Drs Vlad Levchenko and Roger Francey for helpful comments. The State Electricity Commission of Victoria funded visits to CSIRO by KRL, who was otherwise supported by the New Zealand Foundation for Research, Science and Technology.

REFERENCES

Allen, L. H., Boote, K .J., Jones, J .W., Jones, P .H., Valle, R .R., Acock, B., Rogers, H. H. and Dahlman, R. C. 1987. Response of vegetation to rising carbon dioxide: Photosynthesis, biomass, and seed yield of soybean, *Glob. Biogeochem. Cycles* **1**, 1–14.

Andres, R. J., Marland, G., Boden, T. and Bishoff, S. 1996. Carbon dioxide emissions from fossil fuel combustion and cement manufacture 1751–1991 and an estimate of their isotopic composition and latitudinal distribution. In: *The carbon cycle* (ed. T. M. Wigley and D. Schimel). Cambridge University Press, Stanford, in press.

Bacastow, R. B. 1981. Numerical evaluation of the evasion factor. In: *Carbon cycle modelling: SCOPE* **16** (ed. B. Bolin). John Wiley and Sons, Chichester, 95–101.

Broecker, W. S. and Peng, T.-H. 1994. Stratospheric contribution to the global bomb radiocarbon inventory: Model versus observation. *Glob. Biogeochem. Cycles* **8**, 377–384.

Broecker, W. S., Gerard, R. and Ewing, M. 1960. Natural radiocarbon in the Atlantic ocean. *J. Geophys. Res.* **65**, 2903–2931.

Broecker, W. S., Peng, T.-H. and Engh, R. 1980. Modeling the carbon system. *Radiocarbon* **22**, 565–598.

Broecker, W. S., Peng, T.-H., Ostlund, G. and Stuiver, M. 1985. The distribution of bomb radiocarbon in the ocean. *J. Geophys. Res.* **90**, 6953–6870.

Broecker, W. S., Sutherland, S., Smethie, W., Peng, T.-H. and Ostlund, G. 1995. Oceanic radiocarbon: Separation of the natural and bomb components. *Glob. Biogeochem. Cycles* **9**, 263–288.

Craig, S. G. and Holmén, K. J. 1995. Uncertainties in future CO_2 projections. *Glob. Biogeochem. Cycles* **9**, 139–152.

Crane, A. J. 1982. The partitioning of excess CO_2 in a five-reservoir atmosphere-ocean model. *Tellus* **34**, 398–405.

Duffy, P. B. and Caldeira, K. 1995. Three-dimensional model calculation of ocean uptake of bomb ^{14}C and implications for the global budget of bomb ^{14}C. *Glob. Biogeochem. Cycles* **9**, 373–375.

Emanuel, W. R., Killough, G. G., Post, W. M. and Shugart, H. H. 1984. Modeling terrestrial ecosystems in the global carbon cycle with shifts in carbon storage capacity by land-use change. *Ecology* **65**, 970–983.

Enting, I. G. 1982. *Nuclear weapons data for use in carbon cycle modelling*. CSIRO Division of Atmospheric Physics Technical Paper No. 44. Commonwealth Scientific and Industrial Research Organisation (Australia), Melbourne.

Enting, I. G. 1990. Ambiguities in the calibration of carbon cycle models. *Inverse Problems* **6**, L39–L46.

Enting, I. G. 1992. The incompatibility of ice-core CO_2 data with reconstructions of biotic CO_2 sources (II). The influence of CO_2-fertilised growth. *Tellus* **44B**, 23–32.

Enting, I. G. and Lassey, K. R. 1993. *Projections of future CO_2*. CSIRO Division of Atmospheric Research Technical Paper No. 27. Commonwealth Scientific and Industrial Research Organisation (Australia), Melbourne.

Enting, I. G. and Mansbridge, J. V. 1987. The incompatibility of ice-core CO_2 data with reconstructions of biotic CO_2 sources. *Tellus* **39B**, 318–325.

Enting, I. G. and Pearman, G. I. 1987. Description of a one-dimensional carbon cycle model calibrated using techniques of constrained inversion. *Tellus* **39B**, 459–476.

Enting, I. G., Wigley, T. M. L. and Heimann, M. 1994. *Future emissions and concentrations of carbon dioxide: Key ocean/atmosphere/land analyses*. CSIRO Division of Atmospheric Research Technical Paper No. 31. Commonwealth Scientific and Industrial Research Organisation (Australia), Melbourne.

Etcheto, J. and Merlivat, L. 1988. Satellite determination of the carbon dioxide exchange coefficient at the ocean-atmosphere interface: A first step. *J. Geophys. Res.* **93**, 15,669–15,678.

Etheridge, D. M., Steele, L. P., Langenfelds, R. L., Francey, R. J., Barnola, J.-M. and Morgan. V. I. 1996. Natural and anthropogenic changes in atmospheric CO_2 over the last 1000 years from air in Antarctic ice and firn. *J. Geophys. Res.* **101**, 4115–4128.

Fairhall, A. W. and Young, J. A. 1985. Historical ^{14}C measurements from the Atlantic, Pacific, and Indian Oceans. *Radiocarbon* **27**, 473–507.

Francey, R. J., Tans, P. P., Allison, C. E., Enting, I. G., White, J. W. C. and Trolier, M. 1995. Changes in oceanic and terrestrial carbon uptake since 1982. *Nature* **373**, 326–330.

Friedli, H., Lotscher, H., Oeschger, H., Siegenthaler, U. and Stauffer, B. 1986. Ice core records of the $^{13}C/^{12}C$ ratio of atmospheric CO_2 in the past two centuries. *Nature* **324**, 237–238.

Goudriaan, J. and Ketner, P. 1984. A simulation study for the global carbon cycle, including man's impact on the biosphere. *Clim. Change* **6**, 167–192.

Hesshaimer, V., Heimann, M. and Levin, I. 1994. Radiocarbon evidence for a smaller oceanic carbon dioxide sink than previously believed. *Nature* **370**, 201–203.

Houghton, R. A. 1995. Effects of land use change, surface temperature and CO_2 concentration on terrestrial stores of carbon. In: *Biotic feedbacks in the global climate system: will the warming speed the warming?* (ed. G. M. Woodwell and F. T. Mackenzie). Oxford University Press, Oxford, 333–350.

IPCC. 1995. *Climate change 1994: Radiative forcing of climate change and an evaluation of the IPCC IS92 emission scenarios* (ed. J. T. Houghton, L. G. Meira

Filho, J. Bruce, H. Lee, B. A. Callander, E. Haites, N. Harris and K. Maskell). Cambridge University Press, Cambridge.

Jain, A. K., Kheshgi, H. S., Hoffert, M. I. and Wuebbles., D. J. 1995. Distribution of radiocarbon as a test of global carbon cycle models. *Glob. Biogeochem. Cycles* **9**, 153–166.

Keeling, C.D. 1994. Global historical CO_2 emissions. *In: Trends '93: A compendium of data on global change.* ORNL/CDIAC-65. (ed. T. A. Boden, D. P. Kaiser, R. J. Sepanski and F. W. Stoss). Carbon Dioxide Information Analysis Center, Oak Ridge National Laboratory, Oak Ridge, Tenn., U.S.A., 501–504.

Keeling, C. D., Bacastow, R. B., Carter, A. F., Piper, S. C., Whorf, T. P., Heimann, M., Mook, W. G. and Roeloffzen, H. 1989. A three-dimensional model of atmospheric transport based on observed winds. 1. Analysis of observational data. In: *Aspects of climate variability in the Pacific and Western Americas* (ed. D. H. Peterson). American Geophysical Union, Washington D.C., U.S.A., 165–236.

Keeling, C.D., Whorf, T.P., Wahlen, M. and van der Plicht, J. 1995. Interannual extremes in the rate of rise of atmospheric carbon dioxide since 1980. *Nature* **375**, 666–670.

King, A. W., Emanuel, W. R. and Post, W. M. 1992. Projecting future concentrations of atmospheric CO_2 with global carbon cycle models: Importance of simulating historical changes. *Environ. Manage.* **16**, 91–108.

Lassey, K. R., Manning, M. R. and O'Brien, B. J. 1990. An overview of oceanic radiocarbon: Its inventory and dynamics. *Rev. Aquatic Sciences* **3**, 117–146.

Lerman, J. C., Mook, W. G. and Vogel, J. C. 1970. C^{14} in tree rings from different localities. In: *Radiocarbon variations and absolute chronology* (ed. I. Olsson). John Wiley and Sons, New York, 275–301.

Levin, I., Kromer, B., Schoch-Fischer, H., Bruns, M., Münnich, M., Berdau, D., Vogel, J. C. and Münnich, K. O. 1985. 25 years of tropospheric ^{14}C observations in central Europe. *Radiocarbon* **27**, 1–19.

Manning, M. R., Lowe, D. C., Melhuish, W. H., Sparks, R. J., Wallace, G., Brenninkmeijer, C. A. M. and McGill, R. C. 1990. The use of radiocarbon measurements in atmospheric studies. *Radiocarbon* **32**, 37–58.

Marland, G., Andres, R. J. and Boden, T. A. 1994. Global, regional and national CO_2 emissions. In: *Trends '93: a compendium of data on global change.* ORNL/CDIAC-65. (ed. T. A. Boden, D. P. Kaiser, R. J. Sepanski and F. W. Stoss). Carbon Dioxide Information Analysis Center, Oak Ridge National Laboratory, Oak Ridge, Tenn., U.S.A., 505–584.

Neftel, A., Moor, E., Oeschger, H. and Stauffer, B. 1985. Evidence from polar ice cores for the increase in atmospheric CO_2 in the past two centuries. *Nature* **315**, 45–47.

O'Brien, K. 1979. Secular variations in the production of cosmogenic isotopes in the Earth's atmosphere. *J. Geophys. Res.* **84**, 423–431.

Oeschger, H., Siegenthaler, U., Schotterer, U. and Gugelmann, A. 1975. A box diffusion model to study the carbon dioxide exchange in nature. *Tellus* **27**, 168–192.

Rath, H.K. 1988 *Simulation of the global ^{85}Kr and $^{14}CO_2$ distribution by means of a time dependent two-dimensional model of the atmosphere* (in German). PhD Thesis, University of Heidelberg, Germany.

Roeloffzen, J. C., Mook, W. G. and Keeling, C. D. 1991. Trends and variations in stable isotopes of atmospheric carbon dioxide. In: *Stable isotopes in plant nutrition, soil fertility and environmental studies.* STI/PUB/845, IAEA-SM-313/93. International Atomic Energy Agency, Vienna, 601–618.

Schimel, D. S. 1995. Terrestrial ecosystems and the carbon cycle. *Global Change Biology* **1**, 77–91.

Siegenthaler, U. 1983. Uptake of excess CO_2 by an outcrop-diffusion model of the ocean. *J. Geophys. Res.* **88**, 3599–3608.

Siegenthaler, U. and Joos, F. 1992. Use of a simple model for studying ocean tracer distributions and the global carbon cycle. *Tellus* **44B**, 186–207.

Siegenthaler, U. and Oeschger, H. 1978. Predicting future atmospheric carbon dioxide levels. *Science* **199**, 388–395.

Siegenthaler, U. and Oeschger, H. 1987. Biospheric CO_2 emissions during the past 200 years reconstructed by deconvolution of ice core data. *Tellus* **39B**, 140–154.

Stuiver, M. and Quay, P. D. 1980. Changes in atmospheric carbon-14 attributed to a variable sun. *Science* **207**, 11–19.

Suess, H. E. 1955. Radiocarbon concentration in modern wood. *Science* **122**, 415–417.

Wigley, T. M. L. 1993. Balancing the carbon budget. Implications for projections of future carbon dioxide concentration changes. *Tellus* **45B**, 409–425.